EasyChair Preprint

№ 6116

Forced Convection Heat Transfer with Convex Dimples and Cross Flow Jet

Pandaba Patro

EasyChair preprints are intended for rapid dissemination of research results and are integrated with the rest of EasyChair.

July 20, 2021

Proceedings of the 25th National and 3rd International ISHMT-ASTFE Heat and Mass Transfer Conference (IHMTC-2019), December 28-31, 2019, IIT Roorkee, Roorkee, India.

IHMTC2019-HTE-722

Forced Convection Heat Transfer with Convex Dimples and Cross Flow Jet

Pandaba Patro
Department of Mechanical Engineering, VSSUT Burla, Odisha

ABSTRACT

In the present study, computational investigation of flow characteristics and heat transfer from a small rectangular channel has been investigated. A turbulent jet impinges from a nozzle attached to the top wall of the rectangular channel and at the entrance of the rectangular channel, turbulent uniform flow took place. The bottom plate is heated and convex dimples are attached for heat transfer enhancement. Finite volume method with $SST\ \ k-\omega$ turbulence model was used for the numerical simulations. The duct Reynolds number (at the inlet) has been varied in the range of $10000-50000$ and Reynolds number at the nozzle has been varied in the range of $6000-12000$, respectively. It has been shown that the heat transfer rate in the presence of cross-flow is found to be much higher than that without cross-flow. Also, presence of convex dimples augments heat transfer than a plane surface.

Keywords: Heat transfer enhancement; jet impingement; convex dimpled surface; SST k-w model; cross flow

NOMENCLATURE

D_h = hydraulic diameter

I = turbulence intensity

k = turbulent kinetic energy

Nu= Nusselt number

Re_D = Duct Reynolds number

Re_N = Nozzle Reynolds number

T = temperature

u= velocity

λ = thermal conductivity

ρ= density of fluid

ω = specific dissipation rate

INTRODUCTION

The main focus of the present study is heat transfer from a mini rectangular channel and implementation of a suitable method to enhance heat transfer. One of the most prominent industrial applications for this type of studies is electronics cooling. In electronic devices, very small area is available for heat transfer. So, cooling of electronic devices is a great challenge owing to higher operational speed and higher power density. Jet impingement is a good technique which has been used since many decades and examined by many researchers as a method of heat transfer enhancement. Simple jet impingement or forced convection alone is not sufficient to transfer the required heat from the electronic components to safeguard it. There are a number of other techniques to complement jet impingement for the heat transfer enhancement such as cross flow, dimples, ribs, etc. Many researchers have investigated heat transfer prediction through mini-channels experimentally as well as numerically.

Juckerman and Lior [1] had shown that at a given flow velocity, jet impingement produces much higher heat transfer rates compared to a conventional forced convection cooling. This happens because the impingement boundary layers are much thinner, and surrounding fluid becomes turbulent by the impinging fluid. One of the main advantages of the impingement cooling is that it offers a compact hardware arrangement. So, it is suitable for use in mini-channels. Many researchers' [2-6] study show that heat transfer augmentation occurred by the jet impingement on a heated surface. Kerarev and Kozlov [7] investigated the flow past a single hemispherical dimple of 150 mm diameter. They found that heat transfer was enhanced by 1.5 times compared to a plane circle of same imprinted diameter. The heat transfer performance of an array of jet impinging on a flat surface with dimples has been investigated experimentally by

Kanokjaruvijit andMartinez-botas [8]. They showed that the impingement heat transfer performance was better at larger nozzle distance. Chyu et al. [9] investigated the effect of dimple geometry by comparing the heat transfer results for two types of dimples such as hemispherical and tear-drop shaped dimples. The teardrop shaped dimples resulted higher heat transfer rates than the hemi-spherical dimples, but at the cost of a higher pressure drop.

Another approach in practical applications is the hybrid cooling method comprising of a turbulent flow at inlet along with a jet impingement from a nozzle at the top wall. Such interaction results in a rather complex flow field by the generation of coherent vortical structures, and these vortices play a dominant role in the mixing of fluids [10] causing enhancement of heat transfer. Air impingement cooling from a circular nozzle in a cross flow was investigated experimentally [11-12]. They found that the heat transfer coefficients were lower than those reported in the literature for an impinging jet in the absence of cross flow. Different cross flow schemes for micro grooved surface were investigated by Xing et al. [13]. They found that best heat transfer performance was attained at the minimum cross flow. A similar study was conducted by Su and Chang [14] experimentally to study the combined effects of groove and nozzle size on heat transfer enhancement. Liquid Crystal Thermography (LCT) had been implemented by Wang et al. [15] to investigate heat transfer in cross flows. They showed that a more pronounced effect on heat transfer enhancement was found out at a lower velocity ratio. Barik et al [16]. Used different surface protrusions (i.e. Rectangular, Triangular and Trapezoidal Ribs) with cross flow approach in a small rectangular channel numerically. They found that the heat transfer enhancement rate is more in triangular ribs compared to other two ribs. Jet impingement heat transfer by using a rib with cross flow approach using liquid crystal thermography was investigated experimentally by Wang et al. [117]. They showed that at a lower nozzle velocity compared to inlet velocity, heat transfer enhancement was more pronounced

From the literature review, it has been found that the heat transfer enhancement approach from a mini channel with cross flow along with convex dimples on the heated surface has not yet been drawn much attention of researchers. Therefore, an attempt has been made to investigate the heat transfer augmentation by implementing the above hybrid scheme in the present research work. The duct and jet Reynolds number have been varied to study their effects on the heat transfer from a heated surface. Also, the effect of convex dimples on the heated surface will be investigated.

COMPUTATIONAL DOMAIN AND MATHEMATICAL MODELLING

A square duct of cross section 0.03mx0.03m of length 0.67 m has been considered as the computational domain (Fig. 1). At the inlet, air enters at a velocity, U_{in} and atmospheric temperature, T_{∞}. A square nozzle of dimension 0.005mx0.005m is placed at the top wall of the duct, which impinges air to the main duct flow. The bottom plate is heated and is maintained at a constant temperature of 100^0C. Bottom heated surface contains convex dimples (dimensions shown in Fig. 2). The red colour surface is the adiabatic wall. An extra length of 10 times the hydraulic diameter of the duct has been considered upstream as well as downstream to ensure a fully developed flow and to reduce the effect of backflow at the duct exit, respectively. Unstructured meshes have been adopted to mesh the entire surface. X-axis passes through the centre of the duct. The square cross section has one side, b= 0.005 m

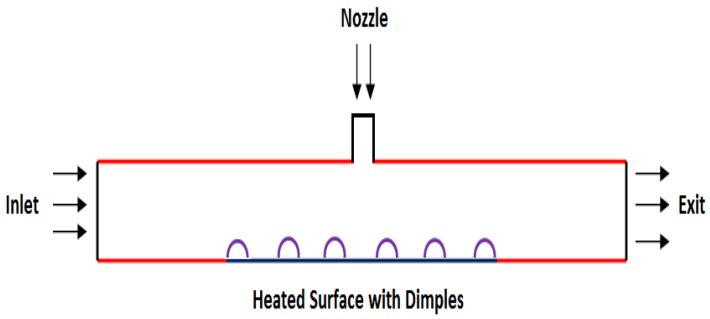

Figure 1. Computational domain

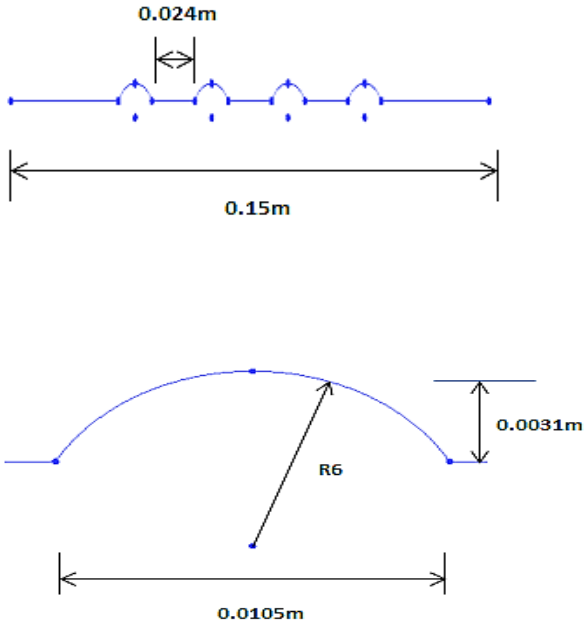

Figure 2. Dimensions for convex dimples

Numerical simulations are performed for a steady, 3-D and turbulent flow. Air is the working fluid and assumed as incompressible. The time averaged governing equations are written as follows:

Continuity equation:

$$\frac{\partial U_i}{\partial x_i} = 0 \qquad (1)$$

Momentum equation:

$$\rho U_j \frac{\partial U_i}{\partial x_j} = -\frac{\partial P}{\partial x_i} + \frac{\partial}{\partial x_j}\left(2\mu S_{ij} - \rho\overline{U_i^{'}U_j^{'}}\right) \quad (2)$$

Energy equations:

$$\rho U_j \frac{\partial T}{\partial x_j} = \frac{\partial}{\partial x_j}\left(\frac{\lambda}{c_p}\frac{\partial T}{\partial x_j} - \rho\overline{T^{'}uU_j}\right) \quad (3)$$

The strain rate tensor is defined as:

$$S_{ij} = \frac{1}{2}\left(\frac{\partial U_i}{\partial x_j} + \frac{\partial U_j}{\partial x_i}\right) \quad (4)$$

Where μ, λ and C_p represents the molecular viscosity, thermal conductivity and specific heat at constant pressure for the working fluid air. Here, air is assumed to be incompressible. P is the mean pressure, T is the mean temperature and U_i is the mean velocity. $T^{'}$ and $U_i^{'}$ are the fluctuating temperature and velocity, respectively. The Reynolds stress ($-\rho\overline{U_i^{'}U_j^{'}}$) and the turbulent heat flux ($-\rho\overline{U_i^{'}T^{'}}$) terms are appeared due to Reynolds time averaging and these terms are closed by using SST $k-\omega$ model (k is turbulence kinetic energy and ω is specific dissipation of turbulence kinetic energy) as follows.

$$-\rho\overline{U_i^{'}U_j^{'}} = 2\mu_t S_{ij} - \frac{2}{3}\rho k\delta_{ij} \quad (5)$$

Where k denotes the turbulent kinetic energy and μ_t is the eddy viscosity.

The turbulent heat flux is defined as:

$$-\rho\overline{U_i^{'}T^{'}} = \frac{\mu_t}{\mathrm{Pr}_t}\frac{\partial T}{\partial x_i} \quad (6)$$

Here, Pr_t denotes the turbulent Prandtl number.

$$\frac{\partial}{\partial x_i}\left(\rho k U_i\right) = \frac{\partial}{\partial x_j}\left[\left(\mu + \frac{\mu_t}{\sigma_\kappa}\right)\frac{\partial k}{\partial x_j}\right] + \min\left(P_\kappa, 10\rho\beta^* k\omega\right) - \rho\beta^* k\omega \quad (7)$$

$$\frac{\partial}{\partial x_i}\left(\rho\omega U_i\right) = \frac{\partial}{\partial x_j}\left[\left(\mu + \frac{\mu_t}{\sigma_\kappa}\right)\frac{\partial \omega}{\partial x_j}\right] + \frac{\alpha\omega}{k}P_\kappa - \rho\beta\omega^2 + 2\left(1-F_1\right)\frac{\rho\sigma_{\omega,2}}{\omega}\frac{\partial k}{\partial x_j}\frac{\partial \omega}{\partial x_j} \quad (8)$$

The eddy viscosity is modelled as:

$$\mu_t = \rho\frac{k}{\omega}\frac{1}{\max\left(\frac{1}{\alpha^*}, \frac{SF_2}{a_1\omega}\right)} \quad (9)$$

The modulus of the mean rate of strain tensor S is defined as $\sqrt{(2S_{ij}S_{ij})}$.

The turbulent viscosity is damped by the coefficient α^*.

$$\alpha^* = \alpha_\infty^*\left(\frac{\alpha_0^* + \frac{\mathrm{Re}_t}{R_k}}{1 + \frac{\mathrm{Re}_t}{R_k}}\right) \quad (10)$$

$$\alpha_0^* = \frac{\beta_i}{3}$$

$$\mathrm{Re}_t = \frac{\rho k}{\mu\omega}$$

The blending functions, F_1 and F_2 are given as

$F_1=\tanh(\emptyset_1^4)$

$F_2=\tanh(\emptyset_2^2)$

$\emptyset_1=\min[\max(\sqrt{\kappa}/0.09\omega y, 500\mu/\rho y^2\omega), 4\rho\kappa/\sigma_{\omega,2}D_\omega^{+}y]$,

$\emptyset_2=\max[2\sqrt{\kappa}/0.09\omega y, 500\mu/\rho y^2\omega]$.

In $\emptyset_1$ and $\emptyset_2$ terms, y is the distance to the next surface. The positive portion of cross-diffusion is represented by $D_\omega^{+} = \max[2\rho/\sigma_{\omega,2}\ \omega\ \partial\kappa/\partial x_j\ \partial\omega/\partial x_j, 10^{-10}]$. The production of turbulence kinetic energy is defined as

$$P_\kappa = -\rho\overline{U_i^{'}U_j^{'}}\frac{\partial U_i}{\partial x_i} \quad (11)$$

For an incompressible flow, term β^* in Eq. (7) is equal to β_1^* which is defined as follows:

$$\beta_1^* = \beta_\infty^*\left(\frac{4/15 + \left(\mathrm{Re}_t/R_\beta\right)^4}{1 + \left(\mathrm{Re}_t/R_\beta\right)^4}\right) \quad (12)$$

Closure constants in SST $k-\omega$ turbulence model are given as follows:

$\alpha_\infty^*=1$, $\beta_\infty^*=0.09$, $\beta_i=0.075$, $\sigma_{\kappa,1}=1.176$, $\sigma_{\omega,1}=2$, $\sigma_{\kappa,2}=1$, $\sigma_{\omega,2}=1.168$, $R_\kappa=6$, $a_1=0.31$ and $R_\beta=8$.

Boundary conditions:

At duct inlet: $U=U_{in}$, $T=T_\infty=300$ K

At nozzle inlet:

V= -V_{in}, T = T_∞=300 K

U_{in} and V_{in} are calculated from the value of the Reynolds number at the duct inlet and nozzle.

Duct Reynolds number, $\mathrm{Re}_D = \frac{\rho U_{in} D}{\mu}$

Nozzle Reynolds number, $\mathrm{Re}_N = \frac{\rho V_{in} d}{\mu}$

Here, D and d are the hydraulic diameter of the duct and nozzle, Respectively.

At adiabatic walls:

U=V=W=0,

For adiabatic wall,

$$q = k\frac{\partial T}{\partial n} = 0$$

For bottom heated wall:

U=V=W=0, T = T_w = 373k

Here U, *V* and W are the velocity components in the x, y, and z direction, respectively.

At duct outlet:

Atmospheric condition is specified. P = P_∞, and T = T_∞

The standard wall function of Launder and Spalding [18] has been used. Wall functions are equations empirically derived and used to satisfy the physics in the near wall region. The first cell center needs to be placed in the log-law region to ensure the accuracy of the results. Wall functions are used to bridge the inner region between the wall and the turbulence fully developed region. When using the wall functions approach, there is no need to resolve the boundary layer causing a significant reduction of the mesh size and the computational domain. In standard wall function, first grid cell needs to be 30 < y+ < 300, where y+ is the non-dimensional distance from the wall to the first grid point.

NUMERICAL METHODOLOGY

The AMG CFD solver ANSYS-Fluent 15.0 was used for carrying out the numerical simulations. The diffusion terms of the governing equations were discretized using the central difference scheme (second-order accurate) and the convective terms were discretized using the upwind scheme (second order accurate). SIMPLE algorithm has been employed for pressure velocity coupling. The convergence criterions for all the equations except the energy equation (10^{-5}) are set to 10^{-3}. SST $k-\omega$ turbulence model along with standard wall function has been used for modelling turbulent stresses. In the present study, the flow separation and its reattachment is expected because of the presence of dimples. Therefore, the SST $k-\omega$ model is preferred over the standard $k-\omega$ and $k-\varepsilon$ models.

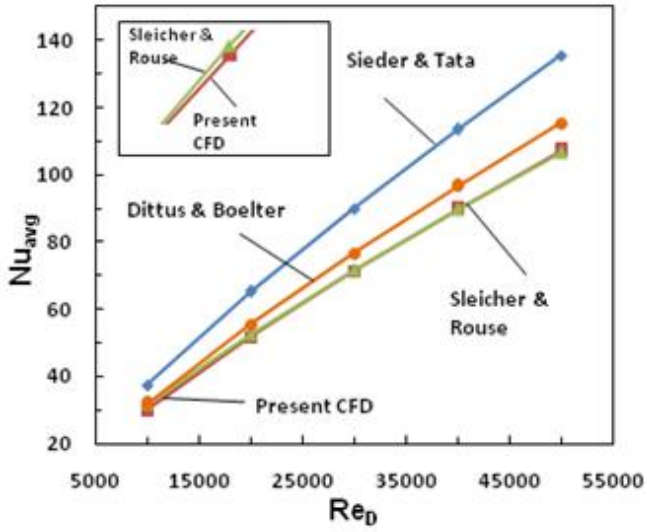

Figure 3. Validation of numerical results

The present numerical scheme is validated with Sleicher and Rouse [19] correlation, Sielder and Tate [20] correlation as well as Dittus-Boelter correlation [21] for a turbulent flow in a 3D pipe (diameter 0.026 m and length 0.67 m). The computed results for average surface Nusselt number with the variation of duct Reynolds number (Re_D) has been shown in figure 3. Predicted surface Nusselt number agreed reasonably well with the correlation by Sleicher and Rouse [19] as shown in figure 3.

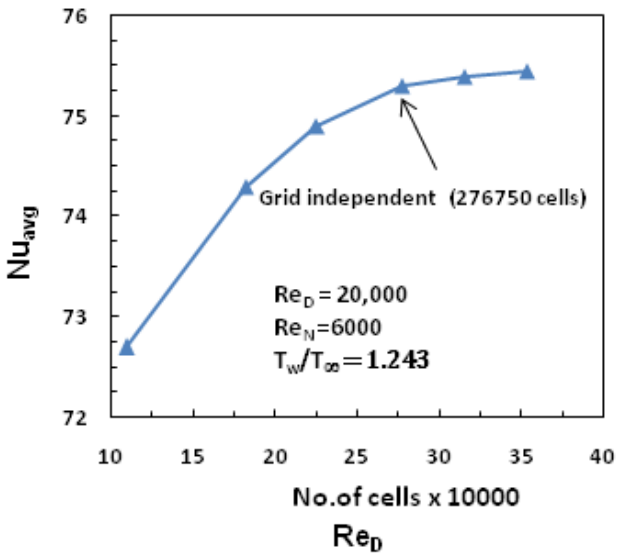

Figure 4. Grid independent test

A grid independent test has also been carried out in figure 4 and it is found that a grid size of 276750 cells is sufficient to carry out the numerical simulations without affecting the accuracy. It can be seen that average Nusselt number (Nu_{avg}

) is increased by 0.53% as the number of cells increase from 225,000 to 276,750. The increase in Nusselt number is insignificant (0.14%) on further increasing the numbers of cells. Thus, 276,750 cells are used as a grid independent mesh for the present study.

RESULTS AND DISCUSSIONS

The effect of duct Reynolds number (Re_D), and nozzle Reynolds number (Re_N) on heat transfer performance of the rectangular channel with cross flow was invetsigated in the presence of dimples on the heated plate and compared with a plane surface (i.e. without dimples). Heat transfer from the heated surface is presented in the form of a non-dimensional number, Nu_{avg}. In all cases, the nozzle was positioned on the centre of the top wall and at an axial distance of X/D=10.57. Figure 5 illustrates the effect of the nozzle Reynolds number (varied in the range 10000 to 50000) on the average Nusselt number. Heat transfer increases with the increase in duct Reynolds number. At Re_N=6000, the Nusselt number was increased by 121% as duct Reynolds number is increased from 10000 to 50000. With respect to nozzle Reynolds number, heat transfer increases with increase in duct Reynolds number but at a reduced rate. It is clear from the figure that at lower duct Reynolds number (i.e. Re_D =10000 and 20000), the Nusselt number has been increased by 59.8% and 32.8% respectively, when the nozzle Reynolds number is increased from 6000 to 12000. At the highest duct Reynolds number (Re_D =50000), the increase of Nusselt number is very less. In the present case, there is only 2.2% increase in heat transfer when nozzle Reynolds number is varied from 6000 to 12000. This concludes that Reynolds number play very important role in the heat transfer prediction in such type of cross flows in mini-channels.

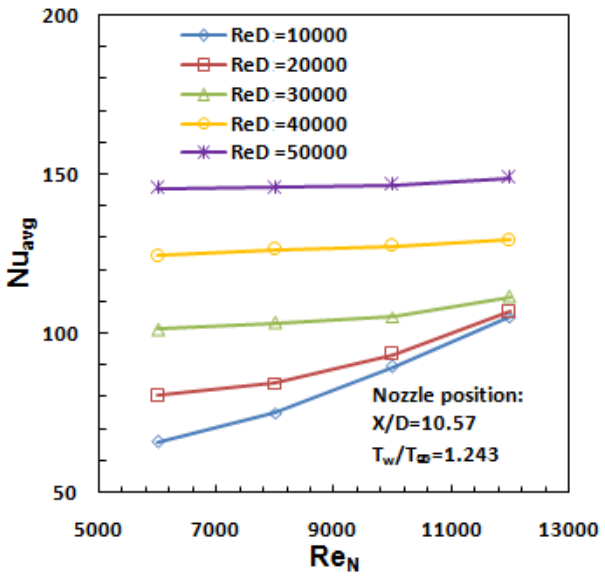

Figure 5. Nusselt number vs. Nozzle Reynolds number

At high duct Reynolds number, high momentum of the duct flow blows away the low momentum fluid from the jet causing the jet fluid not reachable to the hot surface to transfer heat from it. Figure 6 shows the variation of average Nusselt number vs. duct Reynolds number for dimpled heated surface and comparison with plane surface.

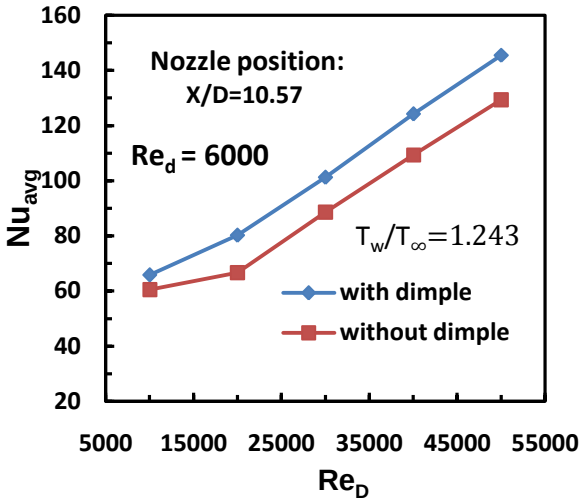

Figure 6. Nusselt number vs. Duct Reynolds number with dimples and without dimples

It is observed that heat transfer increases with the increase in duct Reynolds number. But addition of dimples on the flat plate affects the heat transfer rate considerably. Dimples increase the exposed surface area for heat transfer by the jet. Also, dimples act as obstacle to the main flow causing augmentation in turbulence and hence increases mixing, which results in an increase in heat transfer rate.

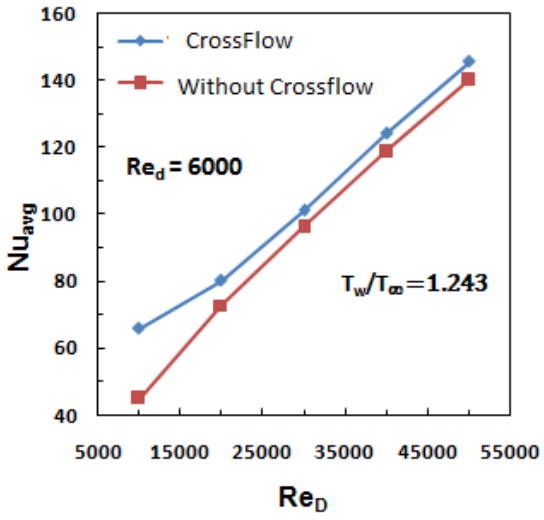

Figure 7. Nusselt number vs. Duct Reynolds number with jet flow and without jet flow

Cross flow effect (i.e. the presence of jet flow) is compared with no cross flow effect on the heat transfer prediction in figure 7. It has been observed form the above plot that at lower duct Reynolds number, cross flow contributes significantly to the enhancement of heat transfer. For Re_D =10000, the Nusselt number is enhanced by 46.5%. For higher values of duct Reynolds number, increase of Nusselt number lies in the range 5-10%. Cross flow increases the turbulence level inside the duct creating stronger recirculation zones. The recirculation zone brings more cold fluid from the duct main stream and

effectively mixes with the hot fluid, thereby increasing heat transfer rate.

CONCLUSIONS

In the present study, we have investigated numerically heat transfer phenomena of a single phase air jet along with a cross flow at inlet for a mini rectangular duct with convex dimples as well as without dimples. Three-dimensional Reynolds averaged Navier-Stokes equations were discretized using finite volume method and solved using AMG solver Fluent 15.0. $SST\ \ k-\omega$ turbulence model with standard wall function was used for the numerical simulations. The major parameters like duct Reynolds number and nozzle Reynolds number were considered to investigate their effect on average heat transfer from the rectangular channel with cross flow and without cross flow as well as with dimples and without dimples. Enhancement of heat transfer is found to be more, when cross flow was used instead of no-cross flow. It was also observed that heat transfer increased significantly by putting convex dimples on the heated surface. Heat transfer increased with increase in duct as well as Nozzle Reynolds numbers.

ACKNOWLEDGEMENTS

This research work is sponsored by the TEQIP-III of Veer Surendra Sai University of Technology (VSSUT) Burla to be presented in IHMTC-2019. The author thanks the TEQIP-III and Mechanical Engineering Department of VSSUT Burla for the timely help.

REFERENCES

1. N. Zuckerman and N. Lior. 2006. "Jet impingement heat transfer: physics, correlations, and numerical modelling." *Advances in heat transfer* 39: 565-631.
2. J. Sakakibara, K. Hishida, M. Maeda. 1997. "Vortex structure and heat transfer in the stagnation region of an impinging plane jet." *International Journal of Heat and Mass Transfer* 40: 3163-3176.
3. R. Gardon, J.C. Akfirat. 1965. "The role of turbulence in determining the heat transfer characteristics of impinging jets." *International Journal of Heat and Mass Transfer* 8: 1261-1272.
4. N. Didden, C.M. Ho. 1985. "Unsteady separation in a boundary layer produced by an impinging jet." *Journal of Fluid Mechanics* 160: 235-256.
5. J. Gauntner, N.B. Livingood, P. Hrycak. 1970. "Survey of Literature on Flow Characteristics of a Single Turbulent Jet Impinging on a Flat Plate." NASA, TN D-5652, Lewis Research Center, USA.
6. C.M. Ho, N.S. Nosseir. 1981. "Dynamics of an impinging jet, part 1: the feedback phenomenon." *Journal of Fluid Mechanics* 105: 119-142.
7. V.S. Kesarev, A.P. Kozlov. 1993. "Convection heat transfer in turbulized flow past a hemispherical cavity." *Heat Transfer Research* 25 (2): 156–160.
8. K. Kanokjaruvijit, R.F. Martinez-botas. 2005. "Jet impingement on a dimpled surface with different cross flow schemes." *International Journal of Heat and Mass Transfer* 48: 161-170.
9. M. K. Chyu, Y. Yu, H. Ding, J. P. Downs, F.O. Soechting. 1997. "Concavity enhanced heat transfer in an internal cooling passage." ASME International Gas Turbine and Aeroengine Congress and Exhibition:. V003T09A080-V003T09A080.
10. M. Salewski, D. Stankovic, L. Fuchs. 2008. "Mixing in Circular and Non-Circular Jets in Crossflow." *Flow, Turbulence and Combustion* 80: 255–283.
11. E. M. Sparrow, R. J. Goldstein, M. A. Rouf. 1975. "Effect of Nozzle-Surface Separation Distance on Impingement Heat Transfer for a Jet in a Cross-flow." *ASME Journal of Heat Transfer* 97: 528–533.
12. J. P. Bouchez, and R. J. Goldstein. 1975. "Impingement Cooling From a Circular Jet in a Cross Flow." *International Journal of Heat and Mass Transfer* 18:. 719–730.
13. Y. Xing, S. Spring, B. Weigand. 2011. "Experimental and numerical investigation of impingement heat transfer on a flat and micro-rib roughened plate with different cross flow schemes." *International Journal of Thermal Science* 50:1293-1307.
14. L.M. Su, S.W. Chang. 2002. "Detailed heat transfer measurements of impinging jet arrays issued from grooved surfaces." *International Journal of Thermal Science* 41: 823-841.
15. L. Wang, B. Sund_en, A. Borg, H. Abrahamsson. 2011. "Control of jet impingement heat transfer in cross flow by using a rib." *International Journal of Heat and Mass Transfer* 54: 4157-4166.
16. A. Barik , A. Mukherjee , P. Patro. 2015. "Heat transfer enhancement from a small rectangular channel with different surface protrusions by a turbulent cross flow jet" *International Journal of Thermal Sciences* 98:. 32-41.
17. L. Wang, B. Sunden, A. Borg, H. Abrahamsson. 2011. "Control of jet impingement heat transfer in cross flow by using a rib." *International Journal of Heat and Mass Transfer* 54: 4157-4166.
18. B.E. Launder, D.B. Spalding. 1974. "The numerical computation of turbulent flows." *Computer Methods in Applied Mechanics and Engineering* 3 (2): 269-289.
19. C.A. Slicher, M.W. Rouse. 1975. "A convenient correlation for heat transfer to constant and variable property fluids in turbulent pipe flow *International Journal of Heat and Mass Transfer* 18: 677-683.
20. E.N. Sieder, and G.E. Tate. 1936. "Heat transfer and pressure drop of liquids in tubes." *Industrial and Engineering Chemistry Research* 28: 1429-1436.
21. F. W. Dittus, L. M. K. Boelter. 1985. "Heat transfer in automobile radiators of the tubular type." Reprinted in *International Communications in Heat and Mass Transfer* 12: 3-22.